



Preparation of Semi IPNs-Hydrogel Composite for Removing Congo Red and Bismarck Brown Y from Wastewater: Kinetic and Thermodynamic Study

Huda Salim Al-Niaem *; Ali Abdulwahid; Whidad Hanoosh

Department of Chemistry, College of Science, University of Basrah, Basrah, Iraq-



CrossMark

Abstract

Modified acrylamide-based semi-interpenetrating polymer network (semi-IPN) hydrogel composites were prepared for Congo red (CR) and Bismarck brown Y (BBY) dyes adsorption from aqueous solutions. Adsorption for both dyes was studied in batch mode and results show adsorption highly dependent on concentration, solution pH, and contact time. The prepared hydrogels exhibited a high adsorption capability. Also, the kinetic studies indicated that the adsorption of dyes followed the pseudo-second-order model and was found to match well with the Langmuir isotherm model. Thermodynamic studies showed that the adsorption process was spontaneous and endothermic. The prepared hydrogel composites also exhibit good regeneration efficiency for the four successive adsorption-desorption cycles. Based on these analyses, it can be concluded that these adsorbents be acted as an efficient option for the removal of contaminant dyes from aqueous solutions.

Keyword: Dye; Hydrogel; Gelatin; Adsorption; Congo red; Bismarck brown Y

1. Introduction

Dyes are color materials of natural or synthetic sources, which resist fading when exposed to heat, light, chemicals, and water [1]. Synthetic materials like plastics, printing, textile, paper, pharmaceuticals, leather, rubber, and paints industries are the main sources of synthetic dye pollution [2][3]. A large amount of untreated dye wastewater was discharged directly into natural water bodies every year [4], impose negative results for both toxicological and esthetical reasons [5]. Dyes when entering the aquatic environment, they decompose into toxic, carcinogenic, or mutagenic compounds because they consist of carcinogens such as benzidine, naphthalene, and other aromatic compounds [6].

Among all the dyestuffs, there are azo dyes that are released in large amounts, directly in water bodies, Azo dyes are considered one of the most harmful categories because they are very persistent in the aquatic environment, due to their chemical composition and their non-biodegradability [7]. The discharge of azo dyes into the natural environment results in the transformation of an azo group to toxic aromatic amines [8] that are highly carcinogenic and mutagenic [9]. The most widely used azo dyes are Congo red (CR) [10]. CR is an anionic or acidic dye [11], exposure can cause allergic reactions and has a

mutagenic and reproductive effect. It can also be metabolized into a human carcinogen called benzidine [12][13]. In the same context, Bismarck Brown Y (BBY) is a cationic or a basic dye, for aquatic organisms, it is poisonous [14]. The abatement of wastewater dyes to a risk-free level is important. It is therefore highly desirable to find an efficient method for the treatment of organic dyes before they are released into the environment [15]. For the treatment of organic dyes, various water treatment techniques. Among these, adsorption has become an effective method to remove dyes due to its high efficiency, simplicity of service, low cost, easy desorption [16], and easy availability of various adsorbents [17]. Many types of adsorbents, such as carbon-based materials [18], polymer composites [19], and hydrogels [20][21] have been described as effective adsorption for toxic dyes. Thus, polymeric hydrogels with high adsorption capacity, sustainability, and recyclability are extremely desirable to purify dyes-polluted wastewater [22].

Hydrogels consist of three-dimensional networks [23], Many hydrogels have a variety of ionic functional groups, such as groups of carboxylic acid, hydroxyl, amine, and sulfonic acid, which make the gels attractive to highly adsorbable charged organic pollutants [24]. Acrylamide-derived hydrogels (AM)

*Corresponding author e-mail: hudaalniaem@gmail.com

Receive Date: 08 March 2021, Revise Date: 02 July 2021, Accept Date: 05 July 2021

DOI: 10.21608/EJCHEM.2021.66511.3438

©2022 National Information and Documentation Center (NIDOC)

have received considerable attention for use as assist carriers in biomedical engineering [25] and as specific adsorbents [26]. Where AM is the most widely used water-soluble product in commercial applications [27].

Nowadays, biopolymer-based hydrogels (e.g., gelatin) have gained intense interest due to their low cost, non-toxic nature, biodegradability, the fact that they do not pose a risk of secondary contamination, and Simplicity of modification [28]. So, the presence of gelatin not only makes the hydrogels more biodegradable and eco-friendlier but also provides more active groups, such as hydroxyl, carboxyl, and amino groups in the structure of hydrogel, which can remove the dyes via electrostatic interaction or π - π interaction and hydrogen bond [29]. Furthermore, graphene oxide (GO) has been used in the hydrogel structure to improve the efficiency of adsorption capacity due to the presence of abundant active groups and its high specific surface area [30]. Also, It is well known that GO is one of the good non-toxic and biocompatible adsorbents [31].

In the present study, hydrogels are prepared based on acrylamide (Am). it was of interest to increase of dye adsorption capacity of AM hydrogels with highly hydrophilic functional groups containing chemical reagents such as gelatin (G) and GO hydrogel for the removal of CR and BBY, a toxic dye, from aqueous solutions by the adsorption method. This present research work will explore the mechanism of adsorption and adsorption kinetics of the dye, and determine the various physicochemical controlling factors on the rate of adsorption and also on the capacity of the adsorbent. The adsorption isotherms will describe by using Langmuir and Freundlich isotherms. Further, this paper also discusses various thermodynamic parameters such as Gibbs free energy change (ΔG°), the heat of adsorption (ΔH°) and entropy change (ΔS°) respectively. Finally, a desorption study is important to clarify the reusability of the prepared adsorbents and to understand the nature of the adsorption system, and evaluate the ability of recycling.

2. Experimental

2.1. Materials and Instruments

All chemicals are of reagent grades and purchased from Sigma-Aldrich Company. They were used without any further purification. The dye solutions

were prepared by dissolving accurately weighed dyes in distilled water. Some characteristics of dyes were given in Table 1. Morphology of the prepared materials was identified using an FEI NOVA NanoSEM 450 field emission scanning electron microscopy (FESEM) under vacuum at an operating voltage of 10 kV. A double beam UV-visible spectrophotometer (T80, PG InL., UK) at 494 and 457 nm was used to determine CR and BBY dyes concentrations.

2.2. Methods

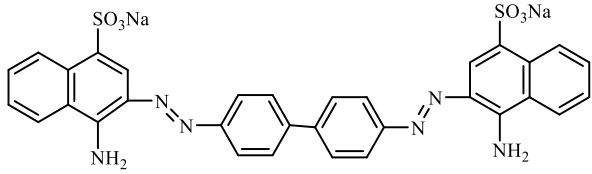
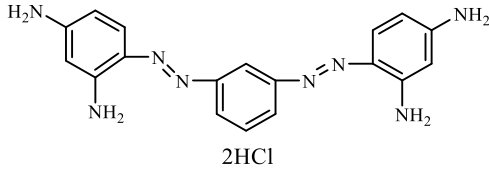
2.2.1. Preparation of graphene oxide (GO)

GO was synthesized from graphite powder according to the modified Hummers' method [32]. 2.0 g of graphite and 1.0 g of NaNO_3 were dissolved in 46.0 ml of concentrated H_2SO_4 (98%) under an ice bath. After about 15 min of stirring, 6.0 g of KMnO_4 was gradually added to the suspension with stirring as slowly as possible to keep the reaction temperature below 20 °C. The suspension was stirred for two hours and then maintained at 35 °C for 30 min. 100.0 mL of deionized water was slowly poured into the suspension, which resulted in a quick increase in temperature, and the temperature should be kept below 98°C. The suspension was further diluted with warm deionized water to approximately 280.0 ml after 15 minutes. 20.0 mL H_2O_2 (30%) was added and the suspension color was changed to a luminous yellow. Then, the suspension was filtered and washed with a warm aqueous solution of 5% aqueous HCl and deionized water, respectively, until no sulfates were detected, and the pH of the filtrate was adjusted to 7. The product, graphene oxide, was dried under a vacuum at 50°C to a constant weight.

2.2.2. Preparation of Acrylamide Hydrogel (AM)

1.0 g of acrylamide (Am), and methylene bis-acrylamide (0.2 g, 20% compared to monomer) were dissolved in 5 mL deionized water. Ammonium persulphate (200 μL of a 10% w/v aqueous solution) was then added to this homogeneous solution and N, N, N', N'-tetramethylethylenediamine (TMEDA) (25 μL). The reaction mixture was stirred for 10 min. at room temperature to complete the polymerization reaction. The resulting hydrogels were dried and washed three times with water to remove any residue of monomers, filtered, and dried under vacuum at 40 °C.

Table 1. Some characteristics of dyes.

Dyes	Molecular Structure	Molar mass (g.mol ⁻¹)	C.I. Nr.
Congo Red (CR)		696.7	22120
Bismarck Brown Y (BBY)		419.31	21000

2.2.3. Preparation of Acrylamide\ Gelatin Semi-IPN hydrogels (AMG)

1.0 g of gelatin (G) was dissolved in 15 mL of distilled water at 45 °C with stirring then 1.0 g of Am and (0.4 g, 20% compared to monomers) of methylene bis-acrylamide as crosslinker in 5 ml distilled water was added with stirring until the solution becomes homogenous. Ammonium persulphate (200 µL of a 10% w/v aqueous solution) was then added to this homogeneous solution and N, N, N', N'-tetramethylethylenediamine (TMEDA) (25 µL). The reaction mixture was stirred for 10 min at room temperature to complete the polymerization reaction. The resulting hydrogels were dried and washed three times with water to remove any residue of monomers, filtered, and dried under vacuum at 40°C.

2.2.4. Preparation of Acrylamide\ Gelatin \Graphene Oxide Composite Hydrogels (AMGGO)

1 g of gelatin (G) was dissolved in 15 mL of distilled water at 45 °C with stirring then 1.0 g of Am and (0.4 g, 20% compared to monomers) of methylene bis-acrylamide as crosslinker in 5 ml distilled water was added with stirring until the solution becomes homogenous then 0.1 g GO was added to the monomer's solution. Ammonium persulphate (200 µL of a 10% w/v aqueous solution) was then added to this homogeneous solution and N,N,N',N'-tetramethyl ethylene diamine (TMEDA) (25 µL). The reaction mixture was stirred for 10 min at room temperature to complete the polymerization reaction. The resulting hydrogels (Fig. 1) were dried and washed three times with water to remove any residue of monomers, filtered, and dried under vacuum at 40°C.

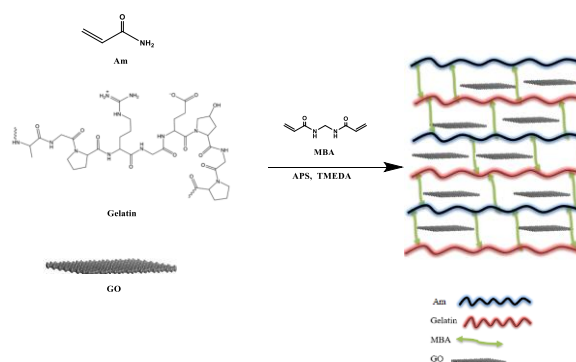


Fig 1. Synthetic routes of preparing AMGGO hydrogel composite.

2.2.5. Preparation of Aqueous Dyes Solutions

A stock solution of dyes (CR, BBY, 1000 mg L⁻¹) was prepared for the adsorption experiments and then the required concentrations were provided with the dilution by using deionized water.

2.2.6. Adsorption experiments

The CR and BBY adsorption capacities of the prepared hydrogels were evaluated using a batch equilibrium procedure. Batch adsorption tests were carried out in stopper flasks containing 25.0 mg of hydrogels and 0.1 L of various amounts of dye solutions (50-12000 mg L⁻¹). The adsorption experiments were carried out on a thermostat shaker for 24 hr. at room temperature (27 °C) at 200 rpm. The residual concentration of dyes remaining in the filtrate was measured by UV-vis spectroscopy at 494 nm and 457 nm for CR and BBY, respectively. A series of isotherms were conducted at various temperatures (25, 45, and 65°C) and pH= (2-12) to study the influence of adsorption isotherms. Adsorption processes were conducted at optimum conditions applying agitation time (60, 45, and 45 min), with a pH of 5.0 for AM, 7.0 for AMS, and

AMSGO of the CR dye, respectively. While agitation time 60 min, with a pH of 5.0 for AM, 6.0 for AMS and AMSGO of the BBY dye, 6.0 for AMS and AMSGO of the BBY dye, respectively.

The amount of the CR and BBY dyes on the prepared adsorbents in the equilibrium (q_e) were calculated from the following Eq. (1)[33]:

$$q_e = \frac{(C_o - C_e)}{W} V \quad (1)$$

where C_o and C_e (mg L^{-1}) are the initial and equilibrium concentrations, respectively of the dye in solution, V (L) is a volume of dyes solution and W (g) is the weight of a hydrogel, and q_e (mg g^{-1}) is the amount of adsorbed dyes per gram of adsorbents (adsorption capacity).

In the analysis of adsorption kinetics and the measurement of kinetic parameters, enthalpy (ΔH°), entropy (ΔS°) and free energy (ΔG°), experiments were performed at (25, 50 and 70 °C) with 25.0 mg of hydrogels in 0.1 L of (400.0, 1000.0 and 1200.0 mg L^{-1}) CR solution for GAM and GAMGO, respectively. While 25.0 mg of hydrogels in 0.1 L (300.0, 600.0, and 750 mg L^{-1}) BBY solution for AM, GAM, and GAMGO, respectively. The maximum adsorption capacity was found at the optimum pH by adjusting the pH of the dye solution from 3.0 to 12.0; the pH of the dye solution was changed using 0.10 M of HCl or NaOH solution.

Desorption of dyes from hydrogels was performed out by applying four times adsorption /desorption experiments under the following criteria: Maximum dye adsorption by applying optimum agitation time, and pH value for each adsorbent using the same adsorbents. Desorption tests were carried out by immersing dye-loaded adsorbent in (1.0 M) NaClO_4 solution, and the mixture was continuously stirred at room temperature for 60 min., then the desorbed dyes were separated by centrifugation and filtration, and spectrophotometrically measured the concentration of dyes [34]. The efficiency of dye desorption removal was calculated by Eq. (2) [35]:

$$S \% = \frac{C_d \cdot V_d}{q_e \cdot m} \cdot 100 \% \quad (2)$$

where S is a dye desorption efficiency, C_d is the concentration of dye in solution after desorption, V_d is the volume of an eluent.

3. Results and discussion

3.1. Characterization of the hydrogels

3.1.1. Field Emission Scanning Electron Microscopy (FESEM)

The morphological feature of the prepared hydrogels has been characterized by recording SEM micrographs which are shown in Fig. 2 (a-c). The hydrogel micrographs demonstrate that they have a porous structure. It has been shown from Fig. 2a that GO shows a layered and wrinkle-like structure that is due to the graphite deformation in the process of exfoliation. The surface also appears somewhat bristly with edge planes, which may enhance the interaction with dyes. In addition, the AM hydrogel showed a smooth and neat surface morphology, as shown in Fig. 2b. Also, It is Been observed, the incorporation of gelatin into AMG hydrogel further increased the porosity (Fig. 2c). On the other hand, the surface morphology of the AMGGO composite hydrogel becomes rougher when GO was added to the AMG hydrogel and the AMSGO shows an irregular, plat-like structure as shown in Fig. 2d. Furthermore, it can be seen that the GO platelets are well distributed as individual platelets in the hydrogel network and no apparent aggregation has been noticed.

3.1.2. Dye Adsorption by the Hydrogel

The anionic (i.e., CR) and cationic (i.e., bismark brown Y) dye adsorption capacity of the prepared hydrogels were investigated. The effects of different variables on the removal of dyes were investigated, such as initial dye concentration, pH, contact time, and temperature, as well as some kinetic, isothermal, and thermodynamic parameters.

3.1.3. Effect of pH on Adsorption

The pH value of the dye solution plays an important factor in the adsorption mechanism as it affects the surface charge of the adsorbent and the protonation degree of the functional groups [36]. The effect of pH on the adsorption capacity of the dye by prepared hydrogels was studied at an optimum initial concentration of both CR and BB dyes. The pH was adjusted between 2.0 and 12.0 by 0.1 M NaOH and 0.1 M HCl solution. The pH effect of CR and BB dyes adsorption capacities in AM, AMS, and AMSGO at 27 °C was demonstrate in Fig. 3 (a and b). It is obvious that the adsorption capacity of both dyes first increases and then decreases with the rise in pH values.

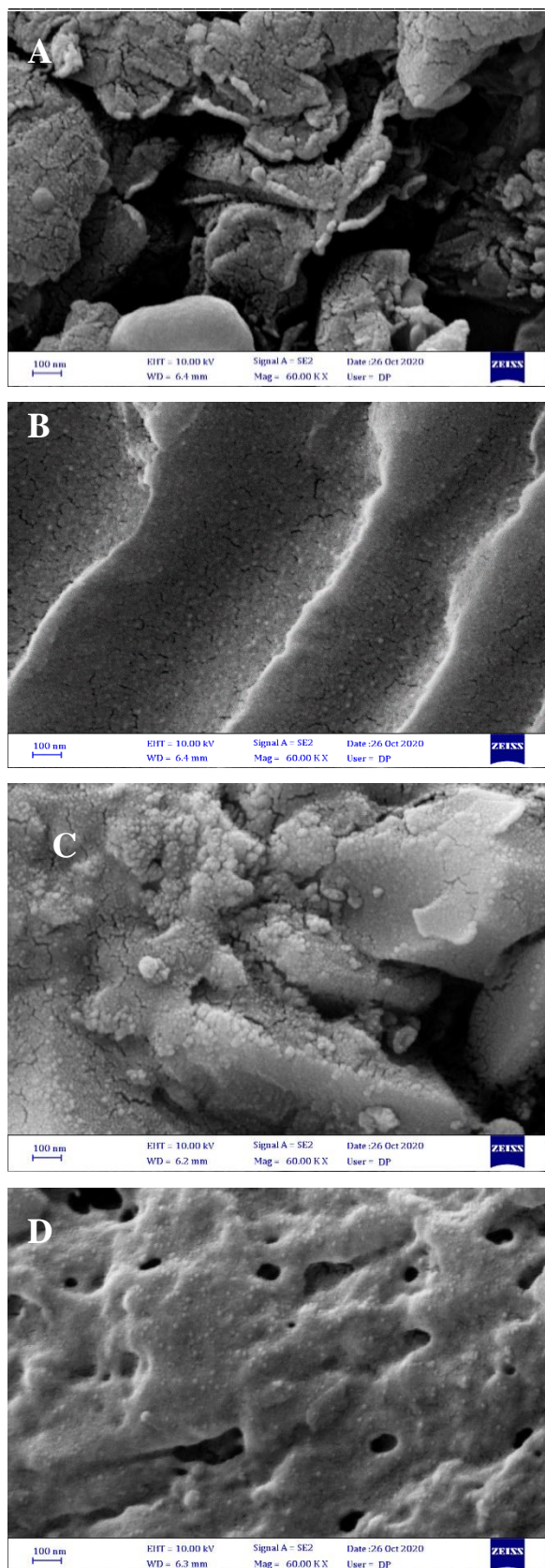


Fig 2. FESEM images of (a) GO, (b) AM, (c) AMG and (d) AMGGO

As the pH value approaches 7, maximum adsorption capacity has been achieved. With pH values rising from 3 to 7, the amino and carboxyl acid groups on the hydrogels were the most suitable groups for the formation of hydrogen bonds between the dyes and the hydrogels. When pH exceeds 9, the adsorption capacity of both CR and BBY dyes decreases, this is due to the repulsion of anionic groups on the hydrogel [37]. The results indicate that the optimum pH value was dependent on the type of adsorbate used for the process of adsorption. (a) Only, the surface of all hydrogels contains different functional groups, such as sulphonic, carboxylic, and amine groups, which can be ionized by changing the pH values of the dye solution.

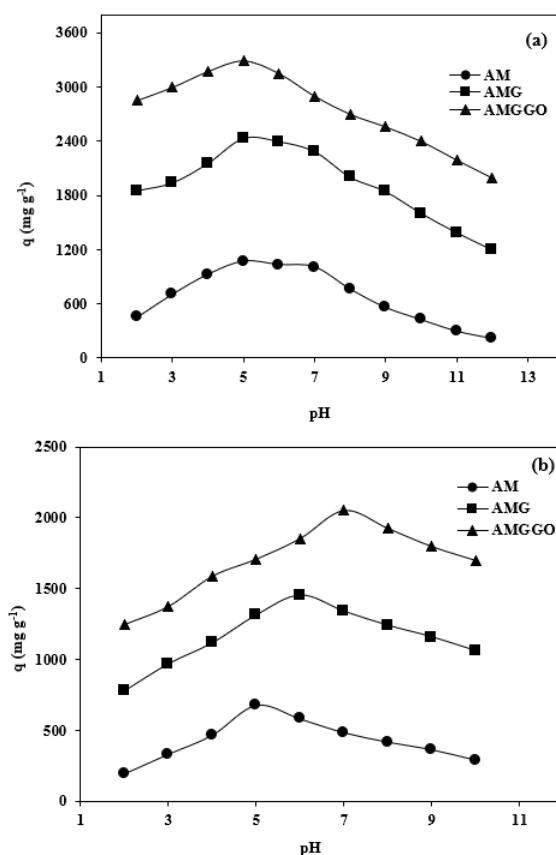


Fig. 3. Effect of pH on the adsorption of (a) CR and (b) BBY dyes onto AM, AMG, and AMGGO at 27 °C

3.1.4. Effect of Time and Temperature on Adsorption

The duration time before the process of adsorption reaches equilibrium called contact time [38]. At the initial concentration of each adsorbent and optimal pH at different temperatures, the effects of contact time on CR and BB dyes adsorption on the prepared hydrogel were investigated. The results are seen in Fig. 4a and 5a, showing that CR and BBY adsorption increased rapidly from 1 to 60 min and that the equilibrium was reached within (60-120 min) for AM hydrogel. Also,

as shown in fig. 4 and 5 (b, c), the optimum contact times for AMG and AMGGO adsorbents were chosen as 45 and 30 min, respectively, for adsorption of CR and BBY dyes, respectively. Generally, the trend for both dyes is more or less the same. Initially, because of the existence of a large number of active sites for adsorption in the hydrogel structure, the adsorption rate of both dyes was higher.

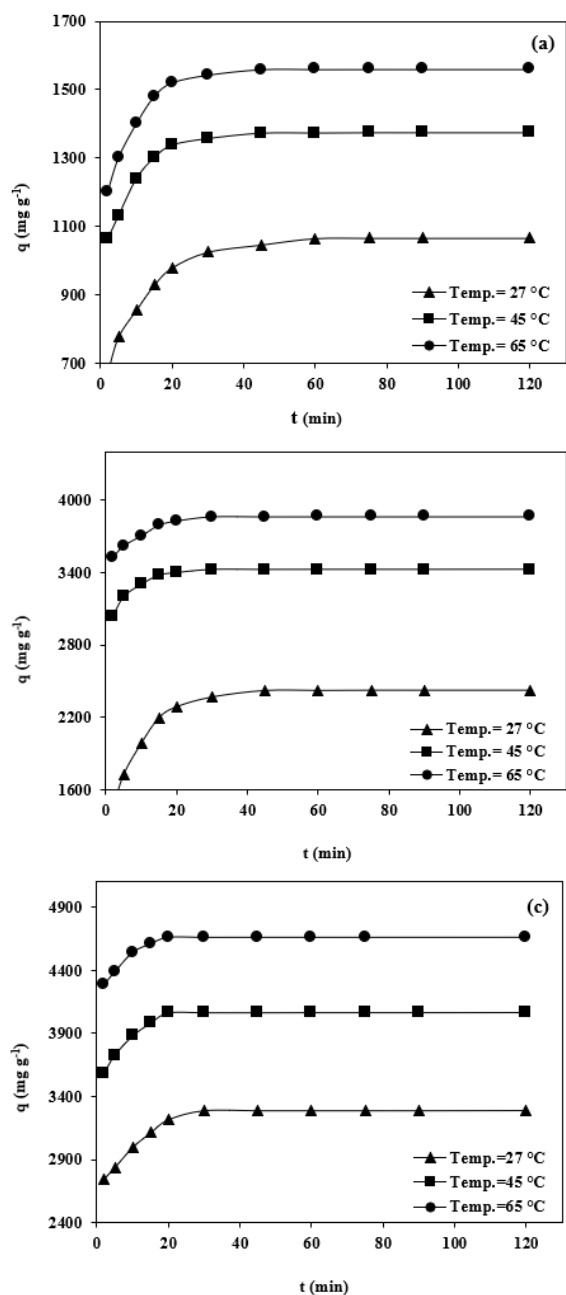


Fig. 4. Effect of time on the adsorption of CR dye onto (a) AM, (b) AMG and (c) AMGGO at 27 °C, 45 °C and 65 °C

Then, due to a decline in the number of adsorption active sites before equilibrium was reached, the adsorption rate decreased gradually. Furthermore, the temperature rises from 27° to 65 °C, and the adsorption capacity for all hydrogels is increased. Since the adsorption of CR and BBY was endothermic, the adsorption capability of the adsorbents is predicted in this pattern. Therefore, for all further experiments, the optimal contact times were selected as 60 min for adsorption of CR and BBY dyes by adsorbent AM; 45 and 30 min for adsorbents AMG and AMGGO, respectively.

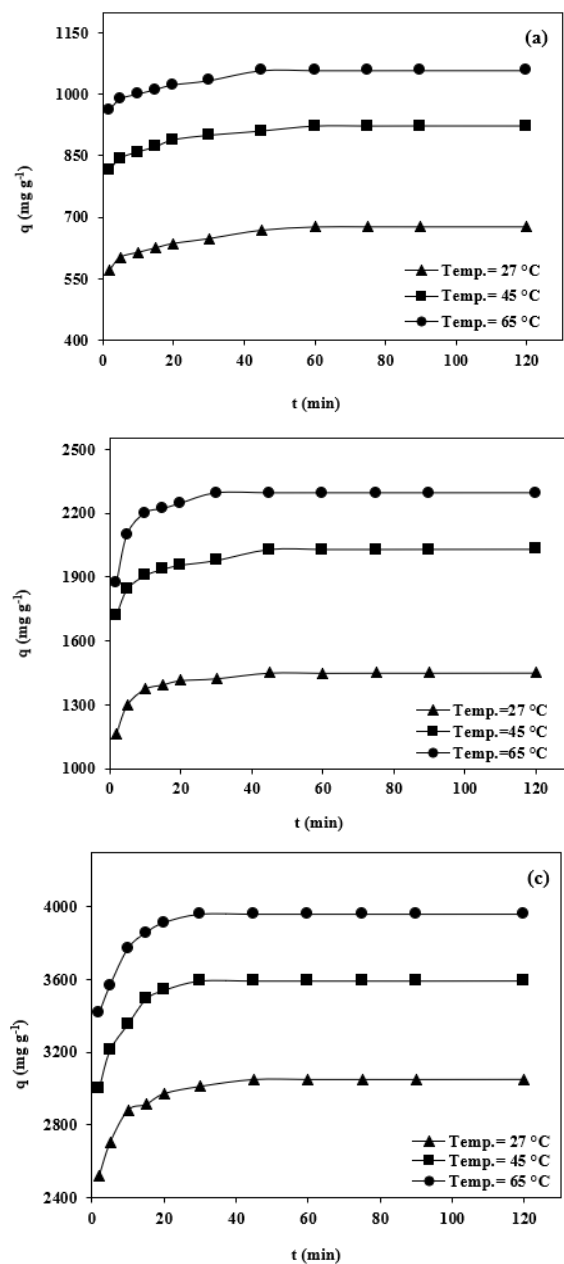


Fig. 5. Effect of time on the adsorption of BBY dye onto (a) AM, (b) AMG and (c) AMGGO at 27 °C, 45 °C, and 65 °C.

3.2. Adsorption Isotherms

The adsorption isotherm can explain the interaction and equilibrium relationship between adsorbed solution and adsorbent at a constant temperature [39]. To find the most appropriate model to describe the adsorption process, the study of isotherm data by fitting it to different models of isotherm is the essential step [40][41]. Adsorption data such as Langmuir and Freundlich isotherms are typically represented as adsorption models [42][43]. The Langmuir model describes the adsorption of adsorbate onto an adsorbent surface and forms a monolayer on the outer surface of the adsorbent. It assumes that there are restricted and homogenous adsorption sites [44]. The Langmuir isotherm is represented by the following equation [45]:

$$\frac{C_e}{q_e} = \frac{1}{(q_{max} \cdot K_L)} + \frac{C_e}{q_{max}} \quad (3)$$

where C_e is the dye concentration remaining in an aqueous solution at equilibrium, q_e is the equilibrium concentration of dyes adsorbed by the hydrogels, q_{max} is the adsorption capacity for monolayer formation of the hydrogel, and K_L represents the Langmuir constant that is related to the apparent energy of adsorption. A plot of C_e/q_e versus C_e should indicate a straight line of slope $(1/q_{max})$ and an intercept of $1/(K_L q_{max})$. The essential characteristics of the Langmuir isotherms can be represented by a separation factor or equilibrium parameter (R_L), which is defined by the following equation [46]:

$$R_L = \frac{1}{1 + (K_L \cdot C_e)} \quad (4)$$

where R_L values indicate the type of adsorption to be irreversible ($R_L=0$), favorable ($0 < R_L < 1$), linear ($R_L=1$) or unfavorable ($R_L > 1$). This is the most commonly used model for isothermal adsorption and has shown good agreement with numerous experimental results [47][48]. The plots of the Langmuir adsorption isotherms of CR and BBY adsorbed on hydrogels AM, AM, and AMGGO are shown in Fig. 6 (a and b), respectively, and Table 2 displays the isothermal constants, q_{max} , K_L , R_L , and the coefficient of correlation (R^2). The Langmuir constant (K_L) provides details on the interaction strength between adsorbed and adsorbed substances. High the K_L value, the stronger will be the interaction and vice versa. So, as shown in Table 2, the K_L value for all

prepared hydrogels is very small, which indicates that the interaction between these hydrogels and dyes is weak [49]. In addition, the R_L for AM, AMG, and AMGGO was determined by using equation 4. The R_L values for all prepared hydrogels lie between 0 to 1 (Table 2), which suggested favorable adsorption of both dyes [50]. Also, the R^2 was closer to unity for both dyes (Table 2) indicating an excellent mathematical fit. So, the adsorption of dyes onto the prepared hydrogels is compatible with the Langmuir isothermal model under the applied optimum conditions, as the active positions of the hydrogel surface are homogeneously distributed [51]. While in the Freundlich model, which is based on the fact that multilayer adsorption occurs on a heterogeneous surface and assumes that the adsorption takes place at sites with varying energy of adsorption [52]. The Freundlich isotherm is represented as follow [53]:

$$\ln q_e = \ln K_F + \frac{1}{n} \ln C_e \quad (5)$$

where K_F is the adsorption capacity, (known as the Freundlich adsorption constant), represents the amount of dyes adsorbed onto hydrogels at equilibrium concentration, while $1/n$ is the adsorption intensity or the surface heterogeneity of the hydrogels (Freundlich parameter). The value of $1/n$ indicates the type of isotherm whether it is favorable ($0 < 1/n < 1$), unfavorable ($1/n > 1$) or irreversible ($1/n = 0$). When the value of n is less than 1, the adsorption involves a chemical process. Otherwise, the adsorption is a physical mechanism [17]. The K_F and $1/n$ values were determined by plotting $\ln q_e$ vs. $\ln C_e$ from the intercept and slope respectively as shown in Fig. 6 and 7 (Table 2), the $1/n$ values are within the $0.1 < 1/n < 1$ range so the adsorption process is favorable. Moreover, in all of these studies, the $1/n$ values for dyes were between 0.1 and 1 indicating that chemisorption was favored by the adsorption of both dyes [54]. Usually, the adsorption mechanism is said to comply with a certain isotherm model, that is to say, the Langmuir or Freundlich isothermal model, if the R^2 value approaches unity [55]. Therefore, as shown in the results shown in Table 2, the dye adsorption by the prepared hydrogels is consistent with the Langmuir isotherm model compared to that of the Freundlich isotherm.

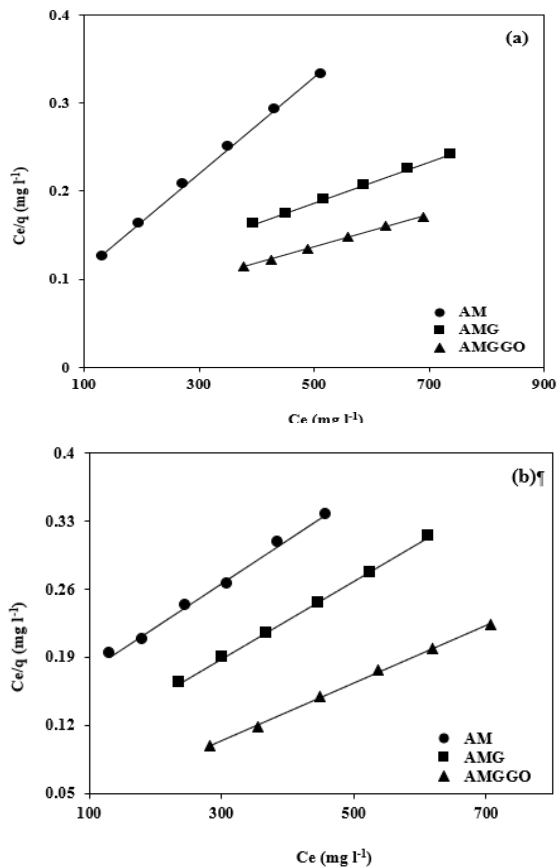


Fig. 6. Langmuir adsorption of (a) CR and (b) BBY dyes onto AM, AMG, and AMGGO at 27 °C.

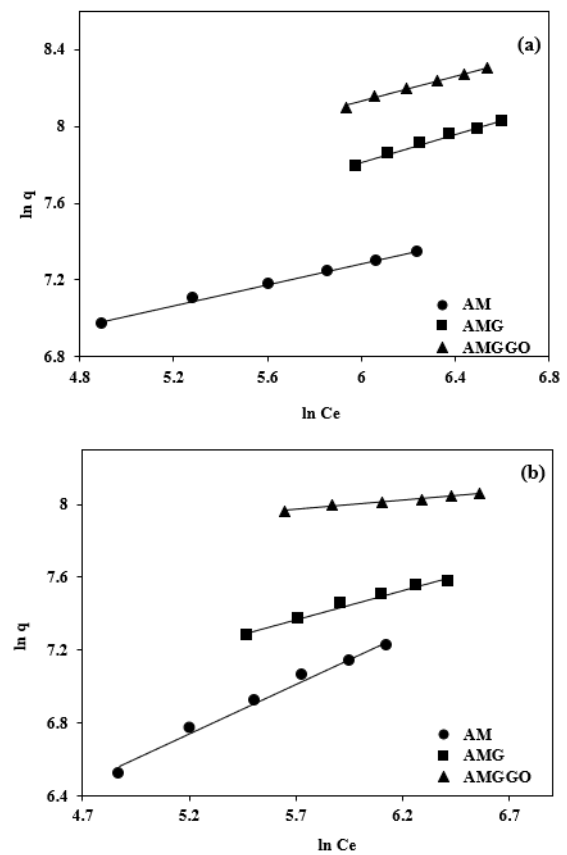


Fig. 7. Freundlich adsorption of (a) CR and (b) BBY dyes onto AM, AMG, and AMGGO at 27 °C.

Table 2. Isotherm parameters for adsorption of dyes by prepared hydrogels

Samples	CR			BBY		
	AM	AMG	AMGGO	AM	AMG	AMGGO
Langmuir						
q_{max} (mg g ⁻¹)	1830.16	4271.68	5437.74	2233.64	2506.89	3381.8
k_L	0.0098	0.0034	0.0041	0.0034	0.0058	0.0193
R_L	0.2027	0.2285	0.1683	0.4933	0.2219	0.0493
R^2	0.9984	0.9994	0.9986	0.9953	0.9994	0.9992
Freundlich						
K_F	286.18	289.76	488.62	49.088	289.76	1638.59
$1/n$	0.2708	0.3573	0.3233	0.5470	0.3573	0.1001
R^2	0.9967	0.9908	0.9885	0.9843	0.9908	0.9596

3.3. Kinetics of Dyes Adsorption

The dye adsorption by the prepared hydrogels are investigated in terms of adsorption kinetics by three different kinetic models, including pseudo-first-order, pseudo-second-order, and intra-particle diffusion, experimental values were introduced, using the following equations [56]:

$$\ln(q_1 - q_t) = \ln q_1 - K_1 t \quad (6)$$

$$\frac{t}{q_t} = \frac{1}{K_2 q_2^2} + \left(\frac{1}{q_2}\right) t \quad (7)$$

$$q_t = k_p t^{1/2} + I \quad (8)$$

where q_t , q_1 , and q_2 are the amounts of dye adsorbed by the prepared hydrogels at various time t , at equilibrium for the pseudo-first-order and pseudo-second-order, respectively. k_1 , k_2 , and k_p are the adsorption rate constants of the pseudo-first-order, pseudo-second-order, and intra-particle diffusion models. C is the intraparticle diffusion constant that relates to the thickness of the boundary layer.

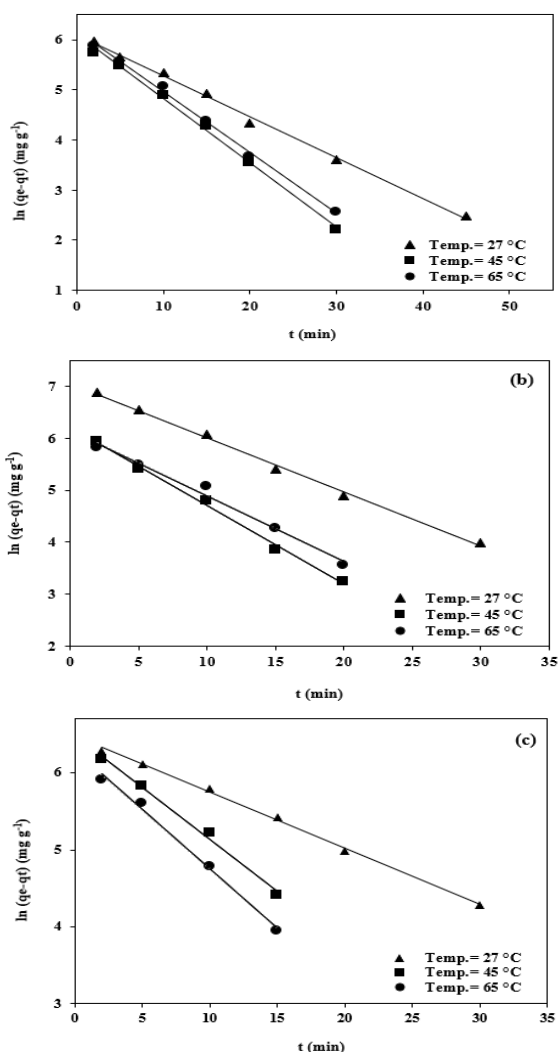


Fig. 8. Pseudo-first order plot for the adsorption of CR dye onto (a) AM, (b) AMG, and (c) AMGGO at 27, 45, and 65 °C.

The experimental data for the adsorption of CR and BBY dyes onto prepared hydrogels under various temperatures were applied in the equations of these models, and the results are shown in Fig. 8-10 and Fig.11-13. The kinetic parameters of kinetic models are summed up in Tables 3 and 4. A high correlation coefficient (R^2) and close accord between the calculated and experimental values (q_1 and q_2) were used to evaluate the fitness of the experimental data to the kinetic models. The pronounced and strong

difference between the experimental absorption capacity and the calculated absorption capacity indicates the deviation from pseudo-first-order kinetics for all the prepared hydrogels for CR and BBY dyes. Whereas the theoretical equilibrium adsorption capacities obtained from the pseudo-second-order model was very well associated with the experimental results and better correlational coefficients ($R^2 > 0.999$) values, thus indicating that the second-order model suited well in comparison with the pseudo-first-order kinetic model [57][58]. In addition, the adsorption rate k values were not always strictly proportional to temperatures. The kinetic model of pseudo-second-order also indicates that the rate determination phase is chemical adsorption. Furthermore, according to Eq. 8, If intraparticle diffusion is the main rate control step, the graph should be linear and pass through the origin. As shown in Fig. 10 and 15, the CR and BBY dye plots did not pass through the origin showing that no intercept was found to be zero. This also implied that the diffusion intraparticle was not the only rate-determining step. Otherwise, it was found from Tables 3 and 4 that k_p values were not always directly proportional to temperatures. As well, the constant values of C were non-zero and increased with rising temperature.

3.4. Thermodynamic of Dyes Adsorption

To evaluate whether the adsorption of prepared hydrogels is an endothermic or exothermic process, the thermodynamic investigation was carried out at various temperatures by calculating the thermodynamic parameters namely, standard free energy (ΔG°), standard enthalpy change (ΔH°) and standard entropy change (ΔS°) using the following equations [59]:

$$K_L = \frac{C_a}{C_e} \tag{9}$$

$$\Delta G^\circ = -RT \ln K_L \tag{10}$$

$$\Delta G^\circ = \Delta H - T\Delta S^\circ \tag{11}$$

$$\ln K_L = \frac{\Delta S^\circ}{R} - \frac{\Delta H^\circ}{R} \frac{1}{T} \tag{12}$$

where K_L is the constant of thermodynamic equilibrium, C_a and C_e are the equilibrium concentrations of CR and BBY on the hydrogel adsorbents and in the solution., respectively. T is the absolute temperature, and R is the gas constant ($8.314 \text{ J molK}^{-1}$).

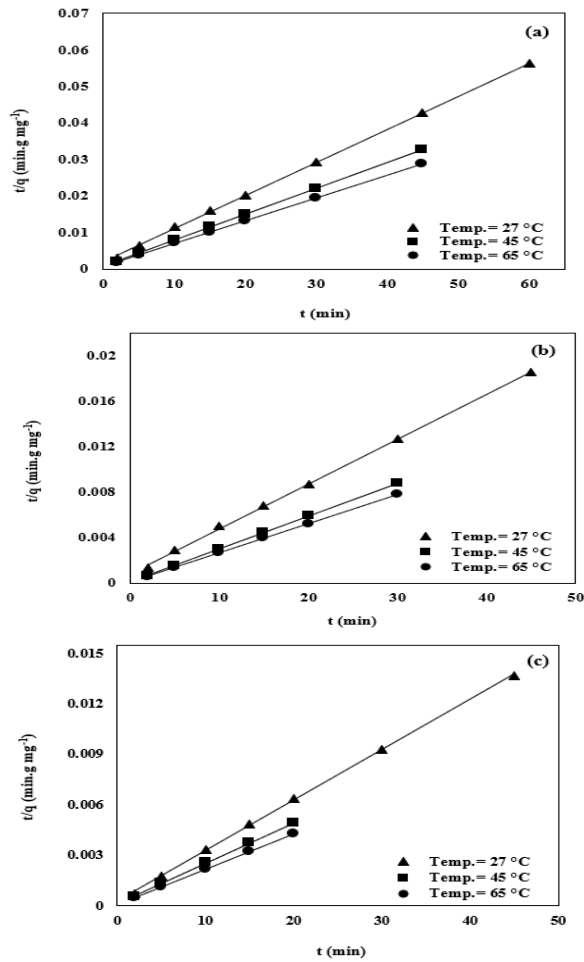


Fig. 9. Pseudo-second order plot for the adsorption of CR dye onto (a) AM, (b) AMG, and (c) AMGGO at 27, 45, and 65 °C.

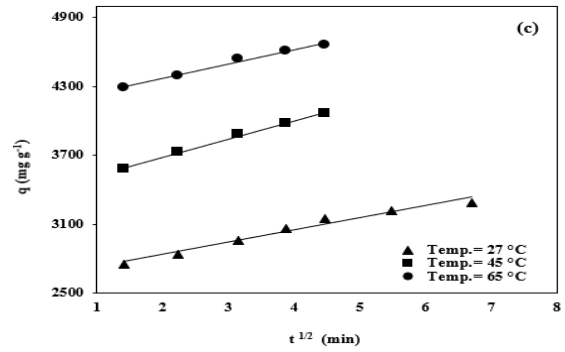
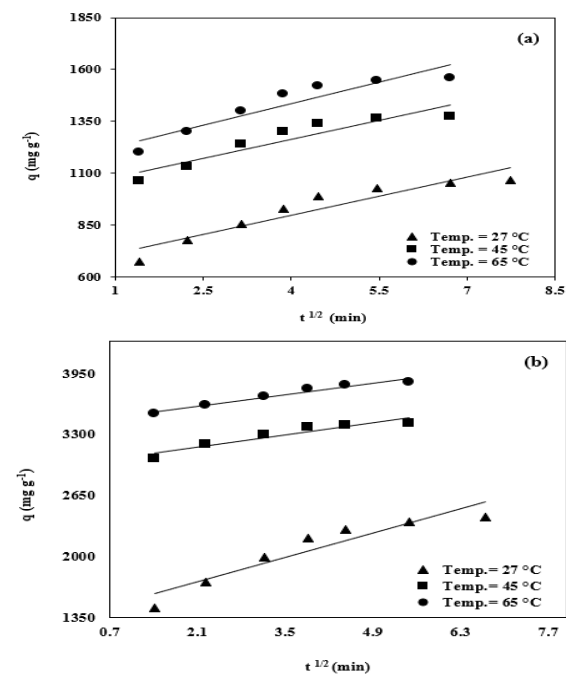


Fig. 10. Intra-particle diffusion plot for the adsorption of CR dye onto (a) AM, (b) AMG, and (c) AMGGO at 27, 45, and 65 °C.

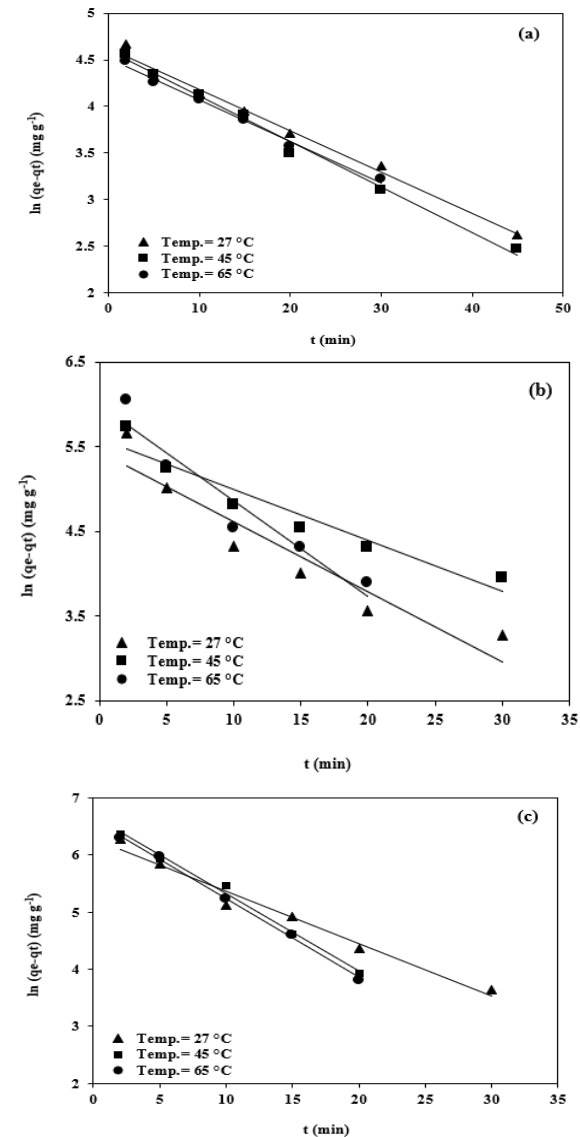


Fig. 11. Pseudo-first order plot for the adsorption of BBY dye onto (a) AM, (b) AMG, and (c) AMGGO at 27, 45, and 65 °C.

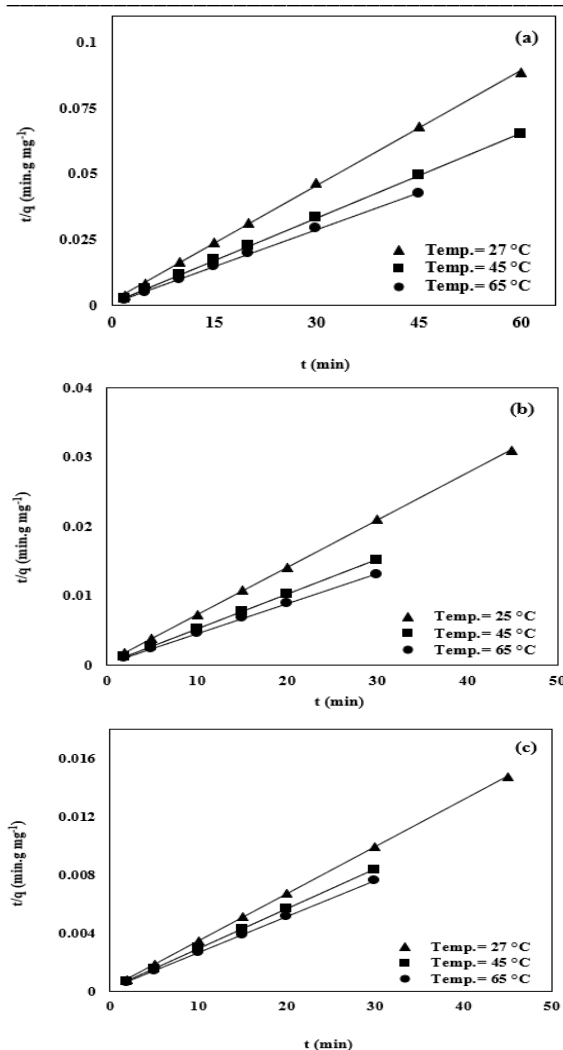


Fig. 12. Pseudo-second order plot for the adsorption of BBY dye onto (a) AM, (b) AMG, and (c) AMGGO at 27, 45, and 65 °C.

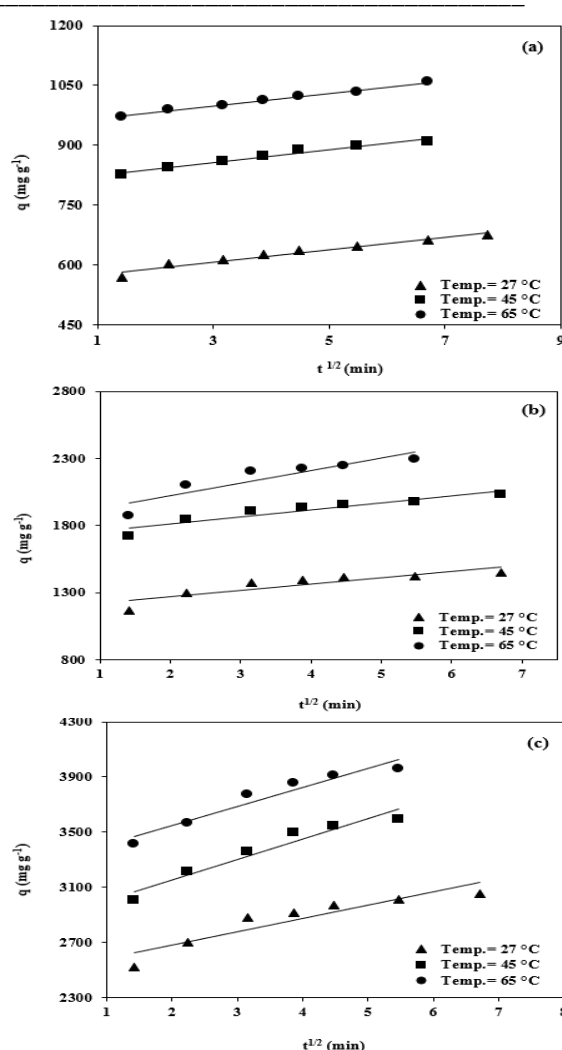


Fig.13. Intra-particle diffusion plot for the adsorption of BBY dye onto (a) AM, (b) AMG, and (c) AMGGO at 27, 45, and 65 °C.

Table 3. Kinetic parameters for adsorption of CR dye by the prepared hydrogels.

	AM			AMG			AMGGO		
<i>T</i> (°C)	25	45	65	25	45	65	25	45	65
<i>q</i> _{max} (Exp.) (mg g ⁻¹)	1065.70	1372.85	1558.98	2424.01	3420.55	3860.04	3290.09	4062.98	4660.89
Pseudo-first order									
<i>q</i> ₁ (Cal.) (mg g ⁻¹)	446.35	447.85	478.02	1169.62	499.49	648.54	648.54	658.57	542.25
<i>K</i> ₁ (min ⁻¹)	0.0819	0.1280	0.1209	0.1045	0.1509	0.1262	0.0726	0.1355	0.1542
<i>R</i> ₁ ²	0.9965	0.9966	0.9972	0.9965	0.9946	0.9867	0.9970	0.9941	0.9943
Pseudo-second order									
<i>q</i> ₂ (Cal.) (mg g ⁻¹)	1102.66	1404.89	1594.39	2535.49	3460.21	3898.64	3337.78	4130.52	4714.76
<i>K</i> ₂ (g mg ⁻¹ min ⁻¹)	1.66E-09	3.78E-10	2.57E-10	6.13E-11	9.15E-12	6.32E-12	2.66E-11	6.80E-12	2.92E-12
<i>R</i> ₂ ²	0.9994	0.9998	0.9998	0.9994	0.9999	0.9999	0.9995	0.9996	0.9999
Intra-particle diffusion									
<i>K</i> _p	61.651	61.413	69.605	185.94	92.78	86.67	106.15	158.25	125.13
<i>C</i>	651.27	1018.9	1157.4	1338.30	2969.10	3420.70	2623.5	3365.8	4118.8
<i>R</i> _p ²	0.8889	0.8791	0.8783	0.8887	0.8965	0.9633	0.9748	0.974	0.9873

Table 4. Kinetic parameters for adsorption of BBY dye by the prepared hydrogels.

<i>T</i> (°C)	AM			AMG			AMGGO		
	25	45	65	25	45	65	25	45	65
<i>q</i> _{max} (Exp.) (mg g ⁻¹)	676.76	921.02	1058.4	1450.90	2020.14	2294.16	3051.22	3592.32	3955.96
Pseudo-first order									
<i>q</i> ₁ (Cal.) (mg g ⁻¹)	107.45	210.51	161.52	228.99	266.89	395.13	537.67	792.88	745.03
<i>K</i> ₁ (min ⁻¹)	0.0819	0.1280	0.1209	0.0826	0.0601	0.1121	0.0919	0.1304	0.1379
<i>R</i> ₁ ²	0.9965	0.9966	0.9972	0.8989	0.9232	0.9211	0.9769	0.9929	0.9956
Pseudo-second order									
<i>q</i> ₂ (Cal.) (mg g ⁻¹)	681.07	925.84	1062.02	3237.29	4130.52	4710.32	3089.28	3660.32	4017.68
<i>K</i> ₂ (g mg ⁻¹ min ⁻¹)	3.17E-09	8.41E-10	4.39E-10	1.9E-11	2.98E-12	2.33E-12	2.36E-11	2.04E-11	1.54E-11
<i>R</i> ₂ ²	0.9995	0.9998	0.9996	0.9995	0.9999	0.9999	0.9999	0.9998	0.9999
Intraparticle diffusion equation									
<i>K</i> _p	15.106	15.055	16.004	47.63	52.39	93.79	95.52	146.94	138.22
<i>C</i>	563.69	810.97	949.50	1174.50	1704.20	1832.30	2492.20	2860.38	3269.80
<i>R</i> _p ²	0.9768	0.9701	0.9935	0.7821	0.8856	0.8259	0.8550	0.9392	0.9354

The graphical representation of the obtained data by plotting $\ln K_L$ versus $1/T$ is shown in Fig.14 (a and b). Thus, the slope and intercept graphs were used to calculate the ΔS° and ΔH° , which presented in Table 5. Also, the ΔG° could be calculated at various temperatures by Eq. (11). In addition, the activation energy (E_a), which can be defined as the minimum amount of energy required to proceed with the adsorption process, was calculated from the Arrhenius equation using the following equation [59]:

$$\ln K = \ln A - \frac{E_a}{RT} \quad (13)$$

where K is the rate constant of the pseudo-second-order kinetic model for adsorption system of CR and BBY dyes since the adsorption analyzes are based on the constant obtained from linearized plots R^2 closest to unity, A is the Arrhenius factor, a straight line with a slope of $-E_a/R$ is obtained by $\ln K$ is graphed versus $1/T$, which as shown in Figure 15.

The determined parameters of thermodynamics are tabled in Table 5. The positive value of ΔS° for the adsorption of CR and BBY dyes on the prepared hydrogels indicates the high degree of randomness of the adsorbed hydrogels and their affinity to the dyes. likewise, for the absorption process of both dyes, the positive value of ΔH° showed that the process was endothermic, accompanied by an increase in absorption capacity of the prepared hydrogels [14][44]. Furthermore, the ΔG° values in all temperatures studied were negative, which underpins the spontaneous nature of adsorption and demonstrates that the adsorption was thermodynamically favorable

[60]. On the one hand, the E_a data for CR and BBY adsorption dyes were obtained and listed in table 5, which confirmed the dominant reaction is the phenomenon of chemisorption. Also, it can be observed that the adsorption of both dyes onto AM have a lower E_a value (less than 40 kJ.mol⁻¹), this result indicated that the adsorption mechanism was physical adsorption, but the modification of AM could have alternated the adsorption mechanism to chemisorption with a higher E_a value [61].

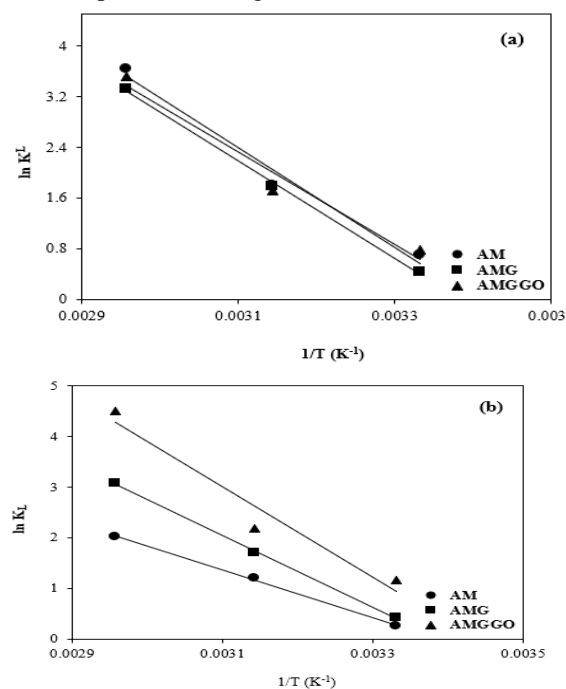


Fig.14. Plots of $\ln K_L$ vs. $1/T$ for estimation of thermodynamic parameters for the adsorption of (a) CR and (b) BBY dyes onto AM, AMG, and AMGGO

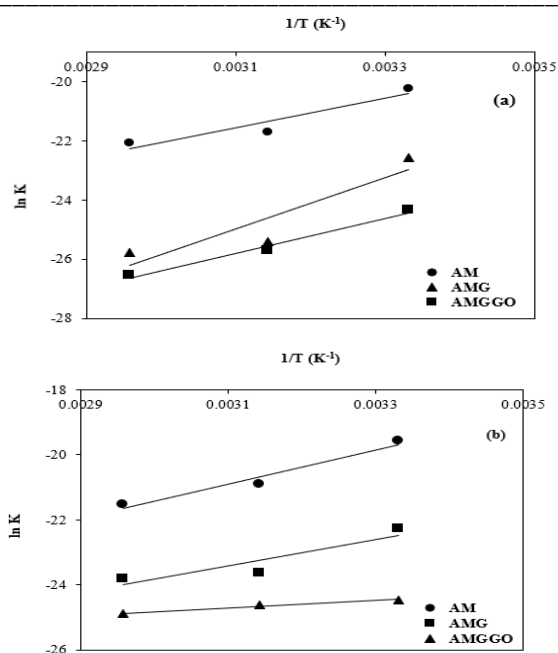


Fig. 15. Plots of $\ln K$ vs. $1/T$ for estimation of activation energy for the adsorption of (a) CR and (b) BBY dyes onto AM, AMS, and AMSGO.

3.5. Desorption Studies

Desorption studies are important to understand the nature of the adsorption mechanism and the recycling spent adsorbent and adsorbate and evaluate the ability of recycling [35]. Adsorbent regeneration might improve the mechanism of adsorption more economically [62]. Thus, successive desorption processes were performed over four consecutive cycles on the CR and BBY dyes to evaluate the reusability of the prepared hydrogels, and results are shown in Table 6, which indicates that the percentage of desorption was good for the four cycles. Therefore, the prepared hydrogels could be used repeatedly with retaining their good adsorption capacity.

Table 5. Thermodynamic parameters for adsorption of dyes by the prepared hydrogels.

Temperature (K)	$-\Delta G^\circ$ (KJ.mol ⁻¹)					
	CR			BBY		
	AM	AMG	AMSGO	AM	AMG	AMGGO
300.15	1.41	0.99	1.57	0.69	1.01	2.36
318.15	5.42	4.89	5.30	3.07	4.60	6.93
338.15	9.87	9.22	9.45	5.71	8.59	12.01
ΔH° (kJ.mol ⁻¹)	65.41	64.08	60.64	38.96	58.88	73.87
ΔS° (J.mol ⁻¹ .K ⁻¹)	222.63	216.77	207.28	132.09	199.53	253.99
E_a (KJ.mol ⁻¹)	38.36	48.25	49.48	32.50	46.67	43.01

Table 6. Four adsorption/desorption cycles of CR and BBY dyes by the prepared hydrogel.

Cycles	CR						BBY					
	AM		AMG		AMGGO		AM		AMG		AMGGO	
	qe	%S	qe	%S	qe	%S	qe	%S	qe	%S	qe	%S
1	1080.2	95.5	3216.2	87.06	4482.7	80.21	676.8	94.2	1450.2	92.4	3051.2	89.9
2	960.3	90.8	3156.9	79.47	4407.2	71.34	663.52	90.4	1415.6	89.1	3015.6	86.4
3	823.5	82.2	3001.4	68.04	4200.3	60.47	612.48	84.7	1368.8	84.3	2971.4	77.8
4	608.1	75.6	2828.1	58.76	4012.4	48.93	559.56	76.5	1293.7	75.6	2900.9	69.1

4. Reference

- [1] Gürses, A., Açıkıldız, M., Güneş, K., and Gürses, M. *S. Dyes and pigments*. Springer (2016).
- [2] Liu, H., and Qiu, H.. Recent advances of 3D graphene-based adsorbents for sample preparation of water pollutants: A review. *Chemical Engineering Journal*, 393, 124691 (2020).
- [3] Shukla, K., Verma, A., Verma, L., Rawat, S., and Singh, J.. A Novel Approach to Utilize Used Disposable Paper Cups for the Development of Adsorbent and its Application for the Malachite Green and Rhodamine-B Dyes Removal from Aqueous Solutions. *Nature Environment and Pollution Technology*, 19(1), 57-70 (2020).
- [4] Ruan, W., Hu, J., Qi, J., Hou, Y., Zhou, C., and Wei, X. Removal of dyes from wastewater by nanomaterials: a review. *Adv Mater Lett*, 10(1), 09-20 (2019).
- [5] Lellis, B., Fávoro-Polonio, C. Z., Pamphile, J. A., & Polonio, J. C.. Effects of textile dyes on health and the environment and bioremediation potential of living organisms. *Biotechnology Research and Innovation*, 3(2), 275-290 (2019).
- [6] Hussain, C. M., and Mishra, A. K. *Nanocomposites for Pollution Control*. CRC Press (2018).
- [7] de Campos Ventura-Camargo, B., and Marin-Morales, M. A. Azo dyes: characterization and toxicity-a review. *Textiles and Light Industrial Science and Technology*, 2(2), 85-103 (2013).
- [8] Ghosh, S. K., Saha, P. D., & Di, M. F.. *Recent Trends in Waste Water Treatment and Water Resource Management*. Springer (2020).
- [9] Hassana, A., Vincent, B. T., Nasiru, I. M., Yakubu, N., Gogo, M. F., and Boko, U. H. Molecular Identification of Azo Dye Degrading Fungi Isolated from Azo Dye Contaminated Soil of Local Dyeing Facility in Bida, Niger State. *Indian Journal of Pure & Applied Biosciences*, 7(4), 1-7 (2019).
- [10] Ismail, M., Akhtar, K., Khan, M. I., Kamal, T., Khan, M. A., M Asiri, A., and Khan, S. B. Pollution, toxicity and carcinogenicity of organic dyes and their catalytic bio-remediation. *Current pharmaceutical design*, 25(34), 3645-3663 (2019).
- [11] Sahoo, J. K., Paikra, S. K., Mishra, M., and Sahoo, H. Amine functionalized magnetic iron oxide nanoparticles: synthesis, antibacterial activity and rapid removal of Congo red dye. *Journal of Molecular Liquids*, 282, 428-440 (2019).
- [12] Fawzy, M. A., & Gomaa, M.. Use of algal biorefinery waste and waste office paper in the development of xerogels: A low cost and eco-friendly biosorbent for the effective removal of congo red and Fe (II) from aqueous solutions. *Journal of environmental management*, 262, 110380 (2020).
- [13] Kalra, A., and Gupta, A. Recent advances in decolorization of dyes using iron nanoparticles: A mini review. *Materials Today: Proceedings*, 36, 689-696 (2021).
- [14] Mizhir, A., Abdulwahid, A., and Al-Lami, H.. Chemical functionalization graphene oxide for the adsorption behavior of Bismarck Brown dye from aqueous solutions. *Egyptian Journal of Chemistry*, 63(5), 1679-1696 (2020).
- [15] Belachew, N., and Bekele, G. Synergy of magnetite intercalated bentonite for enhanced adsorption of congo red dye. *Silicon*, 12(3), 603-612 (2020).
- [16] Ahmed, D. N., Naji, L. A., Faisal, A. A., Al-Ansari, N., and Naushad, M. Waste foundry sand/MgFe-layered double hydroxides composite material for efficient removal of Congo red dye from aqueous solution. *Scientific reports*, 10(1), 1-12 (2020)..
- [17] Kaur, K., Jindal, R., and Saini, D.. Synthesis, optimization and characterization of PVA-co-poly (methacrylic acid) green adsorbents and applications in environmental remediation. *Polymer Bulletin*, 1-22 (2019).
- [18] Azari, A., Nabizadeh, R., Nasser, S., Mahvi, A. H., and Mesdaghinia, A. R. Comprehensive systematic review and meta-analysis of dyes adsorption by carbon-based adsorbent materials: Classification and analysis of last decade studies. *Chemosphere*, 250, 126238 (2020).
- [19] Xie, Z. W., Lin, J. C., Xu, M. Y., Wang, H. Y., Wu, Y. X., He, F. A., and Jiang, H. L. Novel Fe₃O₄ Nanoparticle/ β -Cyclodextrin-Based Polymer Composites for the Removal of Methylene Blue from Water. *Industrial & Engineering Chemistry Research*, 59(26), 12270-12281 (2020).
- [20] Pandey, P. K., Sharma, S. K., and Sambhi, S. S. Kinetics and equilibrium study of chromium adsorption on zeolite NaX. *International Journal of Environmental Science & Technology*, 7(2), 395-404 (2010).
- [21] Wahlström, N., Steinhagen, S., Toth, G., Pavia, H., and Edlund, U. Ulvan dialdehyde-gelatin hydrogels for removal of heavy metals and methylene blue from aqueous solution. *Carbohydrate Polymers*, 249, 116841 (2020).
- [22] Salama, A. Preparation of CMC-gP (SPMA) super adsorbent hydrogels: exploring their capacity for MB removal from waste water. *International journal of biological macromolecules*, 106, 940-946 (2018).
- [23] Rehman, T. U., Shah, L. A., Khan, M., Irfan, M., and Khattak, N. S. Zwitterionic superabsorbent polymer hydrogels for efficient and selective removal of organic dyes. *RSC advances*, 9(32), 18565-18577 (2019).
- [24] Kong, Y., Zhuang, Y., Han, Z., Yu, J., Shi, B., Han, K., and Hao, H. Dye removal by eco-friendly physically cross-linked double network polymer hydrogel beads and their functionalized composites. *Journal of Environmental Sciences*, 78, 81-91 (2019).
- [25] Walia, R., Akhavan, B., Kosobrodova, E., Kondyurin, A., Oveissi, F., Naficy, S., and Bilek, M. M. Hydrogel-Solid Hybrid Materials for Biomedical Applications Enabled by Surface-Embedded Radicals. *Advanced Functional Materials*, 30(38), 2004599 (2020).
- [26] Pashaei-Fakhri, S., Peighambari, S. J., Foroutan, R., Arsalani, N., and Ramavandi, B. Crystal violet dye sorption over acrylamide/graphene oxide bonded sodium alginate nanocomposite hydrogel. *Chemosphere*, 270, 129419 (2021).
- [27] Mollakhalili-Meybodi, N., Khorshidian, N., Nematollahi, A., and Arab, M.. Acrylamide in bread: a review on formation, health risk assessment, and determination by analytical techniques. *Environmental Science and Pollution Research*, 1-19 (2021).
- [28] Ruiz, C., Vera, M., Rivas, B. L., Sánchez, S., and Urbano, B. F.. Magnetic methacrylated gelatin-g-polyelectrolyte for methylene blue sorption. *RSC Advances*, 10(71), 43799-43810 (2020).
- [29] Wu, M., Chen, W., Mao, Q., Bai, Y., & Ma, H. Facile synthesis of chitosan/gelatin filled with graphene bead adsorbent for orange II removal. *Chemical Engineering Research and Design*, 144, 35-46 (2019).

- [30] Scalese, S., Nicotera, I., D'Angelo, D., Filice, S., Libertino, S., Simari, C., and Privitera, V. Cationic and anionic azo-dye removal from water by sulfonated graphene oxide nanosheets in Nafion nanocomposite membranes (2016).
- [31] Chon, J. W., Yang, X., Lee, S. M., Kim, Y. J., Jeon, I. S., Jho, J. Y., and Chung, D. J. Novel PEEK Copolymer Synthesis and Biosafety—I: Cytotoxicity Evaluation for Clinical Application. *Polymers*, 11(11), 1803 (2019).
- [32] da Silva, A. O., Weber, R. P., Monteiro, S. N., Lima, A. M., Faria, G. S., da Silva, W. O., and Pinheiro, W. A. Effect of graphene oxide coating on the ballistic performance of aramid fabric. *Journal of Materials Research and Technology*, 9(2), 2267-2278 (2020).
- [33] Yilmaz, E., Guzel Kaya, G., and Deveci, H.. Removal of methylene blue dye from aqueous solution by semi-interpenetrating polymer network hybrid hydrogel: Optimization through Taguchi method. *Journal of Polymer Science Part A: Polymer Chemistry*, 57(10), 1070-1078 (2019).
- [34] Mohebbali, S., Bastani, D., and Shayesteh, H. Equilibrium, kinetic and thermodynamic studies of a low-cost biosorbent for the removal of Congo red dye: acid and CTAB-acid modified celery (*Apium graveolens*). *Journal of Molecular Structure*, 1176, 181-193 (2019).
- [35] Soldatkina, L., and Zavrichko, M. Equilibrium, kinetic, and thermodynamic studies of anionic dyes adsorption on corn stalks modified by cetylpyridinium bromide. *Colloids and Interfaces*, 3(1), 4 (2019).
- [36] Lafi, R., Montasser, I., and Hafiane, A. Adsorption of congo red dye from aqueous solutions by prepared activated carbon with oxygen-containing functional groups and its regeneration. *Adsorption Science & Technology*, 37(1-2), 160-181 (2019).
- [37] Zhu, L., Guan, C., Zhou, B., Zhang, Z., Yang, R., Tang, Y., and Yang, J. Adsorption of dyes onto sodium alginate graft poly (acrylic acid-co-2-acrylamide-2-methyl propane sulfonic acid)/kaolin hydrogel composite. *Polymers and Polymer composites*, 25(8), 627-634 (2017).
- [38] Mizhira, A. A., Abdulwahid, A. A., and Al-Lamib, H. S.. Adsorption of carcinogenic dye Congo red onto prepared graphene oxide-based composites. *desalination and water treatment*, 202, 381-395 (2020).
- [39] Al-Ghouti, M. A., and Al-Absi, R. S.. Mechanistic understanding of the adsorption and thermodynamic aspects of cationic methylene blue dye onto cellulosic olive stones biomass from wastewater. *Scientific Reports*, 10(1), 1-18 (2020).
- [40] Ayawei, N., Ebelegi, A. N., and Wankasi, D. Modelling and interpretation of adsorption isotherms. *Journal of chemistry*, 2017 (2017).
- [41] Shih, C., Park, J., Sholl, D. S., Realff, M. J., Yajima, T., and Kawajiri, Y. Hierarchical Bayesian estimation for adsorption isotherm parameter determination. *Chemical Engineering Science*, 214, 115435 (2020).
- [42] Dash, B., Dash, B., and Rath, S. S. A thorough understanding of the adsorption of Ni (II), Cd (II) and Zn (II) on goethite using experiments and molecular dynamics simulation. *Separation and Purification Technology*, 240, 116649 (2020).
- [43] Wu, J., Xia, A., Chen, C., Feng, L., Su, X., and Wang, X. Adsorption thermodynamics and dynamics of three typical dyes onto bio-adsorbent spent substrate of *Pleurotus eryngii*. *International journal of environmental research and public health*, 16(5), 679 (2019).
- [44] Abdulwahid, A. A., Alwattar, A. A., Haddad, A., Alshareef, M., Moore, J., Yeates, S. G., and Quayle, P. An efficient reusable perylene hydrogel for removing some toxic dyes from contaminated water. *Polymer International* (2021).
- [45] Langmuir, I. The adsorption of gases on plane surfaces of glass, mica and platinum. *Journal of the American Chemical Society*, 40(9), 1361-1403 (1918).
- [46] Gautam, R. K., Mudhoo, A., Lofrano, G., and Chattopadhyaya, M. C. Biomass-derived biosorbents for metal ions sequestration: Adsorbent modification and activation methods and adsorbent regeneration. *Journal of environmental chemical engineering*, 2(1), 239-259 (2014).
- [47] Foo, K. Y., and Hameed, B. H.. Insights into the modeling of adsorption isotherm systems. *Chemical engineering journal*, 156(1), 2-10 (2010).
- [48] Sulaymon, A. H., Mohammed, T. J., and Al-Najar, J. Equilibrium and kinetics studies of adsorption of heavy metals onto activated carbon. *Canadian Journal on Chemical Engineering & Technology*, 3(8), 86-92 (2012).
- [49] Rehman, T. U., Bibi, S., Khan, M., Ali, I., Shah, L. A., Khan, A., and Ateeq, M. Fabrication of stable superabsorbent hydrogels for successful removal of crystal violet from waste water. *RSC Advances*, 9(68), 40051-40061 (2019).
- [50] Abdellatif, F. H. H., and Abdellatif, M. M. Bio-based i-carrageenan aerogels as efficient adsorbents for heavy metal ions and acid dye from aqueous solution. *Cellulose*, 27(1), 441-453 (2020).
- [51] Saber-Samandari, S., Saber-Samandari, S., Joneidi-Yekta, H., and Mohseni, M. Adsorption of anionic and cationic dyes from aqueous solution using gelatin-based magnetic nanocomposite beads comprising carboxylic acid functionalized carbon nanotube. *Chemical Engineering Journal*, 308, 1133-1144 (2017).
- [52] Hussain, C. M. *Nanomaterials in chromatography: current trends in chromatographic research technology and techniques*. Elsevier (2018).
- [53] Freundlich, H. The uptake of substances on solid surfaces. *Physicse Chemical Society*, 40, 1361-1368 (1906).
- [54] Saber-Samandari, S., Gulcan, H. O., Saber-Samandari, S., and Gazi, M. Efficient removal of anionic and cationic dyes from an aqueous solution using pullulan-graft-polyacrylamide porous hydrogel. *Water, Air, & Soil Pollution*, 225(11), 1-14 (2014).
- [55] Bello, K., Sarojini, B. K., & Narayana, B. Design and fabrication of environmentally benign cellulose based hydrogel matrix for selective adsorption of toxic dyes from industrial effluvia. *Journal of Polymer Research*, 26(3), 1-13 (2019).
- [56] Ugbe, F. A., and Abdus-Salam, N. Kinetics and thermodynamic modelling of natural and synthetic goethite for dyes scavenging from aqueous systems. *Arabian Journal of Chemical and Environmental Research*, 7(1), 12-28 (2020).
- [57] Utsev, J. T., Iwar, R. T., and Ifyalem, K. J. Adsorption of methylene blue from aqueous solution onto delonix regia pod activated carbon: batch equilibrium isotherm, kinetic and thermodynamic studies. *agricultural wastes*, 4(5), 18-19 (2020).
- [58] Ahmadi, S., and Mostafapour, F. K. Adsorptive removal of aniline from aqueous solutions by *Pistacia atlantica* (Baneh) shells: isotherm and kinetic studies.. *Journal of Science, Technology and Environment Informatics* 5(1), 327-335 (2017).

-
- [59] Erdem, M., Yüksel, E., Tay, T., Çimen, Y., and Türk, H. Synthesis of novel methacrylate based adsorbents and their sorptive properties towards p-nitrophenol from aqueous solutions. *Journal of colloid and interface science*, 333(1), 40-48 (2009).
- [60] Murcia-Salvador, A., Pellicer, J. A., Fortea, M. I., Gómez-López, V. M., Rodríguez-López, M. I., Núñez-Delicado, E., and Gabaldón, J. A.. Adsorption of Direct Blue 78 using chitosan and cyclodextrins as adsorbents. *Polymers*, 11(6), 1003 (2019).
- [61] Chakraborty, S., Mukherjee, A., Das, S., Maddela, N. R., Iram, S., and Das, P. Study on isotherm, kinetics, and thermodynamics of adsorption of crystal violet dye by calcium oxide modified fly ash. *Environmental Engineering Research*, 26(1), 210-222 (2021).
- [62] Al-Rubayee, W. T., Abdul-Rasheed, O. F., and Ali, N. M. Preparation of a modified nanoalumina sorbent for the removal of alizarin yellow R and methylene blue dyes from aqueous solutions. *Journal of Chemistry*, 2016 (2016).